Journal of Solid State Chemistry 182 (2009) 77–82

Contents lists available at ScienceDirect

Journal of Solid State Chemistry

journal homepage: www.elsevier.com/locate/jssc

A group of new selenite-chlorides of strontium and *d*-metals (Co,Ni): Synthesis, thermal behavior and crystal chemistry

Peter S. Berdonosov *, Andrey V. Olenev, Alexei N. Kuznetsov, Valery A. Dolgikh

Department of Chemistry, Moscow State University, GSP-1, Leninskie Gory, 1 Build. 3, 119991 Moscow, Russia

ARTICLE INFO

Article history:
Received 20 August 2008
Received in revised form
21 September 2008
Accepted 2 October 2008
Available online 14 October 2008

Keywords:
Selenite
Crystal structure
ELF
Lone electron pair

ABSTRACT

The new selenite-chlorides with composition $Sr_3(SeO_3)_2Cl_2$ (**I**) and $Sr_2M(SeO_3)_2Cl_2$ (M = Co, Ni (**II** and **III**)) were obtained. They crystallize in monoclinic system **I**: space group $C2/m$, $a = 13.203(2)$ Å, $b = 5.5355(8)$ Å, $c = 6.6170(10)$ Å, $\beta = 95.89(1)^\circ$, $Z = 2$; **II** Space group $P2_1/n$, a = 5.3400(10) Å, b = 6.4279(6) Å, $c = 12.322(1)$ Å, $\beta = 92.44(1)^\circ$, $Z = 2$; **III**: space group $P2_1/n$, $a = 5.3254(11)$ Å, b = 6.4363(13) Å, $c = 12.197(2)$, $\beta = 92.53(3)^\circ$, $Z = 2$. All three compounds are constructed in the same manner. Sr polyhedra form infinite layers, which are interconnected into a 3D framework by means of Sr polyhedra in the case of I or Co and Ni polyhedra in the case of **II** and **III**. Se atoms are situated inside the channels of the 3D framework. The topological analysis of ELF for **I** confirmed that the lone electron pairs of SeO_3 groups are located inside these channels.

1. Introduction

Metal selenites and tellurites attract a significant attention due to their ability to adopt a variety of structures where the lone electron pair of Se(IV) or Te(IV) ions may act as an invisible structure-guiding agent [1–3]. Selenium compounds that contain SeO_3E pyramids are frequently regarded as compounds that may exhibit non-centrosymmetric structures and consequently possess certain nonlinear optical properties [2]. On the other hand, the last decade saw several new experimental works, where *d*-metal containing selenites and tellurites were examined in order to obtain low-dimensional structures which could contain *d*-metal ions with different kind of spin–spin interactions and promising low temperature magnetic properties (for example, [4–7]).

Recently, we have described the crystal structure of the strontium selenite (selenate (IV)) $SrSeO_3$ [8]. The 3D framework of this compound is composed of SrO_9 polyhedra and contains channels where SeO_3 groups are located. This structure seems to be a good matrix for incorporation of different ions resulting in new compounds. Indeed, when our work was in progress, the synthesis and crystal structure of a similar new compound $Sr_3(SeO_3)(Se_2O_5)Cl_2$ was reported [9]. To the best of our knowledge there are no other strontium selenite halides known.

In the present work we describe the synthesis, crystal structure determination, thermal properties, and IR spectra of the new Sr selenites chlorides: $Sr_3(SeO_3)_2Cl_2$, $Sr_2Co(SeO_3)_2Cl_2$, and $Sr_2Ni(SeO_3)_2Cl_2$. In addition, a quantum chemical approach was used in order to estimate the Se(IV) lone pair chemical activity for $Sr_3(SeO_3)_2Cl_2$.

2. Experimental section

2.1. Synthesis

$SrSeO_3$ was obtained by the technique described in [8]. Anhydrous strontium chloride was obtained from chemically pure $SrCl_2 \cdot 6H_2O$ by calcination under open-air conditions at 200–400 °C. Cobalt and nickel chlorides were obtained by chlorination of chemically pure metals by a slow flow of anhydrous chlorine at 750–800 °C. The purity of obtained samples was confirmed by the powder X-ray diffraction using STOE STADI-P diffractometer (Ge curved monochromator, Cu$K\alpha$1 radiation) and utilizing PDF-2 file [10] as a reference.

Thus synthesized $SrSeO_3$ was mixed with anhydrous chloride in ratios 2:1, 1:1 and 1:2, ground in agate mortar and quickly loaded into the quartz tubes. The tubes were sealed under vacuum ($\sim 10^{-2}$ Torr) and placed into an electronically controlled furnace and heated at 750–800 °C for 5–8 days. After heating, the furnace was cooled down to 550 °C within four days and after that switched off.

Samples appeared as powders containing a small amount of crystals being white for pure Sr sample, blue for Co and yellow for Ni.

* Corresponding author. Fax: +7 495 939 0998.
E-mail address: berdonosov@inorg.chem.msu.ru (P.S. Berdonosov).

0022-4596/$ - see front matter © 2008 Elsevier Inc. All rights reserved.
doi:10.1016/j.jssc.2008.10.003

2.2. X-ray diagnostics

The analysis of the X-ray powder patterns has shown the formation of new compounds in the $SrSeO_3/MCl_2$ (M = Sr, Co,Ni) mixtures. The patterns obtained for the samples with high MCl_2 content may be considered as a sum of a new compound pattern and starting MCl_2 or their hydrated forms. The patterns obtained for $2SrSeO_3{:}1MCl_2$ samples were similar in the case of Co and Ni, and different for the Sr compound. The better quality single crystals were found in 1:1 reaction mixtures and they were used for the structure determination.

2.3. Structure determination

Suitable single crystals of **I**, **II** and **III** were mounted on a CAD 4 (Nonius) goniometer head for structure determination. Monoclinic unit cell parameters for all compounds were refined based on 24 well-centered reflections in the angular range $18.3^\circ<\theta<19.1^\circ$ (**I**), $16.3^\circ<\theta<18.1^\circ$ (**II**) and $16.3^\circ<\theta<17.8^\circ$ (**III**). All data sets were collected at the ambient temperature in ω–2θ mode with the data collection parameters listed in Table 1. A semiempirical absorption correction was applied to the data based on ψ-scans of not less than five reflections having their λ angles close to 90°. For **I** analysis of systematic reflection absences revealed that the monoclinic unit cell was C-centered and for the structure determination the most symmetric possible space group $C2/m$ was chosen. For **II** and **III** analysis of the systematic extinctions unambiguously pointed at the space group $P2_1/n$. For all the structures positions of all atoms except oxygen were found by direct methods (SHELXS-97) [11]. Oxygen positions were found by a sequence of $\Delta\rho(xyz)$ synthesis and least-squares cycles. Final anisotropic refinement on F^2 (SHELXL-97) [11] lead to $R1 = 0.0382$, $wR2 = 0.0999$ (**I**); $R1 = 0.0430$, $wR2 = 0.1150$ (**II**) and $R1 = 0.0502$, $wR2 = 0.1695$ (**III**). Atomic coordinates and isotropic thermal parameters are summarized in Tables 2 and 3. Further details of the crystal structure investigation(s) may be obtained from Fachinformationszentrum Karlsruhe, 76344 Eggenstein-Leopoldshafen, Germany (fax: (+49)7247 808 666; e-mail: crysdata@fiz-karlsruhe.de, http://www.fiz-karlsruhe.de/request_for_deposited_data.html) on quoting the appropriate CSD numbers (419617 for $Sr_3(SeO_3)_2Cl_2$ (**I**), 419615 for $Sr_2Co(SeO_3)_2Cl_2$ (**II**) and 419616 for $Sr_2Ni(SeO_3)_2Cl_2$ (**III**)).

2.4. Thermal analysis

Thermal analysis for the obtained substances was performed using the Q-1500 derivatograph (MOM, Hungary). Substances were heated under the open air conditions in small alumina crucibles from room temperature to 1000 °C with 10°/min heating ratio.

Table 2
Atomic coordinates ($\times 10^4$) and equivalent isotropic displacement parameters ($A^2 \times 10^3$) for $Sr_3(SeO_3)_2Cl_2$, $Sr_2Co(SeO_3)_2Cl_2$ and $Sr_2Ni(SeO_3)_2Cl_2$

Atom	Site	Occupancy	x	Y	z	U (eq)[a]
$Sr_3(SeO_3)_2Cl_2$						
Sr (1)	4*i*		2879 (1)	0	7847 (1)	10 (1)
Sr (2)	4*g*	0.5	0	230 (20)	0	16 (1)
Se	4*i*		4039 (1)	0	12667 (1)	10 (1)
Cl	4*i*		1600 (1)	0	3767 (2)	17 (1)
O (1)	8*j*		1423 (2)	2662 (6)	8830 (4)	16 (1)
O (2)	4*i*		4745 (3)	0	7724 (8)	34 (1)
$Sr_2Co(SeO_3)_2Cl_2$						
Co	2*b*		−5000	5000	0	8 (1)
Sr	4*e*		121 (1)	3012 (1)	2330 (1)	11 (1)
Se	4*e*		−53 (1)	7633 (1)	754 (1)	7 (1)
Cl	4*e*		4590 (2)	8302 (2)	−1068 (1)	15 (1)
O (1)	4*e*		−2531 (6)	6228 (6)	1199 (3)	11 (1)
O (2)	4*e*		2224 (6)	5800 (6)	1050 (3)	12 (1)
O (3)	4*e*		533 (7)	9264 (6)	1780 (3)	15 (1)
$Sr_2Ni(SeO_3)_2Cl_2$						
Ni	2*b*		−5000	5000	0	8 (1)
Sr	4*e*		135 (2)	3012 (2)	2331 (1)	11 (1)
Se	4*e*		−56 (2)	7611 (2)	736 (1)	8 (1)
Cl	4*e*		4613 (5)	8243 (4)	−1039 (2)	14 (1)
O (1)	4*e*		−2571 (14)	6233 (13)	1204 (6)	9 (1)
O (2)	4*e*		2244 (14)	5804 (13)	1052 (6)	11 (2)
O (3)	4*e*		501 (15)	9280 (14)	1756 (7)	14 (2)

[a] U (eq) is defined as one-third of the trace of the orthogonalized Uij tensor.

Table 1
Crystal data and structure refinement parameters for $Sr_3(SeO_3)_2Cl_2$, $Sr_2Co(SeO_3)_2Cl_2$ and $Sr_2Ni(SeO_3)_2Cl_2$

Formula	$Sr_3(SeO_3)_2Cl_2$	$Sr_2Co(SeO_3)_2Cl_2$	$Sr_2Ni(SeO_3)_2Cl_2$
Diffractometer		CAD−4	
Temperature (K)		293(2)	
Crystal system		Monoclinic	
Space group	$C2/m$	$P2_1/n$	$P2_1/n$
Cell parameters			
a (Å)	13.203 (2)	5.3400 (10)	5.3254 (11)
b (Å)	5.5355 (8)	6.4279 (6)	6.4363 (13)
c (Å)	6.6170 (10)	12.3220 (10)	12.197 (2)
β (deg)	95.890 (10)	92.440 (10)	92.53 (3)
Cell volume (Å^3)	481.05 (12)	422.57 (9)	417.66 (15)
Z		2	
Calculated density (g/cm^3)	4.057	4.393	4.697
Absorption coefficient (mm^{-1})	24.684	23.750	19.318
Wavelength		Mo$K\alpha$	
Crystal size (mm)			
Theta range for data collection (deg)	3.09–29.91	3.17–32.49	3.17–29.95
Reflections collected	824	3180	1378
Data/restraints/parameters	760/0/40	1517/0/63	1215/6/63
Goodness-of-fit on F^2	1.109	1.066	1.192
Final R indices	$R1 = 0.0382$	$R1 = 0.0430$	$R1 = 0.0502$
[$I>2\sigma(I)$]	$wR2 = 0.0999$	$wR2 = 0.1150$	$wR2 = 0.1695$
Largest diff. peak and hole eA^{-3}	1.357 and −2.782	3.878 and −1.742	2.581 and −1.716
ICSD number	419617	419615	419616

Table 3
Bond lengths (Å) for $Sr_3(SeO_3)_2Cl_2$, $Sr_2Co(SeO_3)_2Cl_2$ and $Sr_2Ni(SeO_3)_2Cl_2$

$Sr_3(SeO_3)_2Cl_2$			$Sr_2Co(SeO_3)_2Cl_2$			$Sr_2Ni(SeO_3)_2Cl_2$		
Bond		Distance	Bond		Distance	Bond		Distance
Sr (1)–O (2)		2.474 (4)	Sr–O (3)		2.515 (4)	Sr–O (3)		2.512 (9)
Sr (1)–O (1)	x2	2.559 (3)	Sr–O (1)		2.593 (3)	Sr–O (1)		2.566 (8)
Sr(1)–O (1)	x2	2.635 (3)	Sr–O (3)		2.650 (4)	Sr–O (3)		2.660 (8)
Sr (1)–Cl		3.0346 (16)	Sr–O (2)		2.666 (3)	Sr–O (2)		2.661 (8)
Sr (1)–Cl	x2	3.0701 (8)	Sr–O (2)		2.788 (4)	Sr–O (2)		2.760 (8)
Sr (2)–O (1)	x2	2.499 (7)	Sr–O (1)		2.838 (4)	Sr–O (1)		2.845 (8)
Sr (2)–O (1)	x2	2.643 (8)	Sr–Cl		3.0208 (14)	Sr–Cl		3.030 (3)
Sr (2)–O (2)	x2	3.043 (11)	Sr–Cl		3.1047 (13)	Sr–Cl		3.145 (3)
Sr (2)–O (2)	x2	3.263 (11)	Sr–Cl		3.3880 (14)	Sr–Cl		3.369 (3)
Sr (2)–Cl	x2	3.0998 (16)	Co–O (2)	x2	2.074 (3)	Ni–O (2)	x2	2.057 (8)
			Co–O (1)	x2	2.093 (3)	Ni–O (1)	x2	2.072 (8)
			Co–Cl	x2	2.5020 (12)	Ni–Cl	x2	2.446 (3)
Se–O (2)		1.651 (4)	Se–O (3)		1.662 (4)	Se–O (3)		1.661 (8)
Se–O (1)	x2	1.704 (3)	Se–O (1)		1.712 (3)	Se–O (2)		1.720 (8)
			Se–O (2)		1.721 (3)	Se–O (1)		1.724 (7)

The strontium containing sample is stable at open air up to 880 °C where endothermic effect was observed and mass loss has begun. Total weight loss for 2 $SrSeO_3$:1 $SrCl_2$ sample is 37.7%.

For the sample with composition 2 $SrSeO_3$:1 $NiCl_2$ two steps of decomposition were observed. First step at 570–870 °C with 20.2% weight loss and second one from 870–1000 °C with 19.8 weight % loss.

Cobalt sample 2 $SrSeO_3$:1 $CoCl_2$ started to decompose at 540 °C and in total lost 39.8% of weight up to 1000 °C.

The Co- and Ni-containing compounds after DTA were studied by the X-ray powder analysis. In the case of cobalt compound the powder pattern was not found to contain known compounds. For the product of nickel compound decomposition, the strong lines of cubic NiO were observed in the X-ray pattern together with the reflections from an unidentified substance.

DTA has shown no effects up to the beginning of decomposition for all three compounds, allowing us to assume that no phase transformations occur in that temperature range.

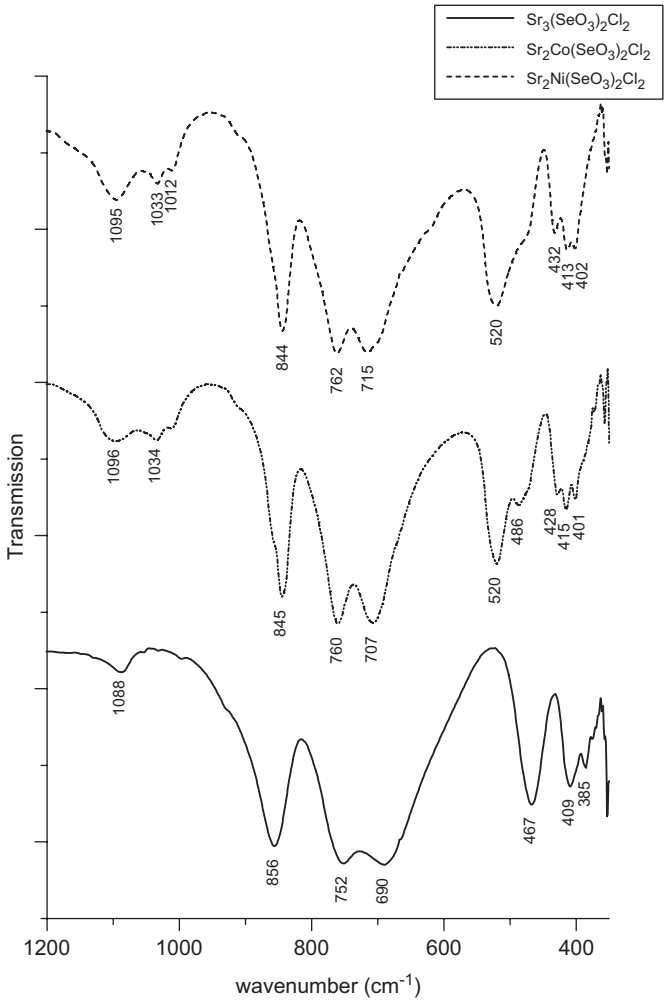

Fig. 1. IR transmission spectra for $Sr_3(SeO_3)_2Cl_2$ and $Sr_2M(SeO_3)_2Cl_2$ (M = Co,Ni).

2.5. IR-diagnostic

IR spectra were collected using PerkinElmer FT-IR spectrometer spectrum one in 4000–350 cm^{-1} range. The samples were pressed into 0.5 mm thick pellets with KBr (Aldrich, for FTIR analysis), with the substance content of 0.25–0.5 mass %. All the compounds turned out to be transparent in the 4000–1100 cm^{-1} range. Transmission IR spectra in the 1200–350 cm^{-1} range are presented in Fig. 1.

2.6. Quantum chemical procedure

The electronic structure of $Sr_3(SeO_3)_2Cl_2$ was calculated on the density functional theory level using a hybrid density functional (B3LYP), employing the CRYSTAL98 program [12]. All calculations included a converged SCF run, with the convergence threshold set at 10^{-7}. An idealized model of the $Sr_3(SeO_3)_2Cl_2$ crystal structure was used in the calculations, where Sr2 y coordinate was set to 0 in order to eliminate splitting of the strontium position into two ones with partial occupancies. All-electron split-valence 6-311G basis sets were used for the selenium and chlorine atoms, and all-electron split-valence 6-21G basis sets were used for the oxygen. Hay and Wadt, small-core (HAYWSC) pseudopotentials were applied to the strontium atoms and the corresponding valence basis set of triple-zeta quality was used as given in Ref. [13].

Electron localization function (ELF) distribution $\eta(r)$ was calculated using the TOPOND98 program [14] based on the results of the SCF calculations. The topology of the ELF surface was investigated using the gOpenMol package [15].

3. Results and discussion

All the new selenites we have synthesized are stable phases. The thermal decomposition of $Sr_3(SeO_3)_2Cl_2$ at 880 °C may be described as a loss of two SeO_2 molecules. The theoretical weight loss 36.8% is in good agreement with observed 37.7%. This model of decomposition agrees well with the thermal decomposition data for $Sr_3(SeO_3)(Se_2O_5)Cl_2$ [9] where the second step of decomposition, observed above 770 °C, may be attributed to the decay of $Sr_3(SeO_3)_2Cl_2$.

Co and Ni compounds are found to decompose in the same manner. The first step of $Sr_2Ni(SeO_3)_2Cl_2$ decomposition (starts at 570 °C) is the loss of one SeO_2 molecule. Theoretical loss 19.8% is in good agreement with the observed 20.2%. The second step is the loss of a second SeO_2 molecule. Total weight loss 39.7% is in good agreement with theoretical 40%. For cobalt compound it is not possible to divide decomposition in two steps, but total weight loss 39.8% agrees with calculated 39.6%. It is clear that compounds with d-metals start to decompose at lower temperatures than $Sr_3(SeO_3)_2Cl_2$.

The data presented in Tables 1–3 show that new compounds may be divided into two groups based on their structure types: $Sr_3(SeO_3)_2Cl_2$ and $Sr_2M(SeO_3)_2Cl_2$ (M = Co,Ni).

The $Sr_3(SeO_3)_2Cl_2$ crystal structure (Fig. 2) contains two crystallographically independent metal positions, Sr1 and Sr2. Sr1 has eight neighbors: five oxygen atoms at the distances 2.49–2.63 Å and three chlorine atoms at the distances 3.04–3.09 Å (Fig. 3a). Bond valence sum calculations (*BVS*) for Sr1 using constants listed in [16] lead to 1.73 if only one closest chlorine atom at the distance 3.04 Å is taken into account. If two more distant 3.09 chlorine atoms are considered, *BVS* becomes 2.16. According to *BVS* estimation, Sr1 has $[Sr(1)O_5Cl_3]$ a distorted square antiprism polyhedron with four oxygen atoms forming one base and three chlorine atoms and one oxygen atom, the other (Fig. 3a). Half occupied 4*g* position of Sr2 splits the ideal 2*a* site of the C2/*m* space group. The Sr2 atom has four oxygen neighbors at the 2.499–2.643 Å distances plus two further oxygen atoms at 3.043 Å and two chlorine atoms at 3.099 Å. Such coordination with two chlorine atoms may be described as a distorted octahedral $[Sr(2)O_4Cl_2]$. *BVS* estimations for such coordination lead to a very low value of 1.59 for Sr2. Due to this reason, two oxygen atoms at the distances of 3.043 Å should be taken into account, and finally Sr2 polyhedron may be described as a two-capped octahedron $[Sr(2)O_{(4+2)}Cl_2]$ (Fig. 3b).

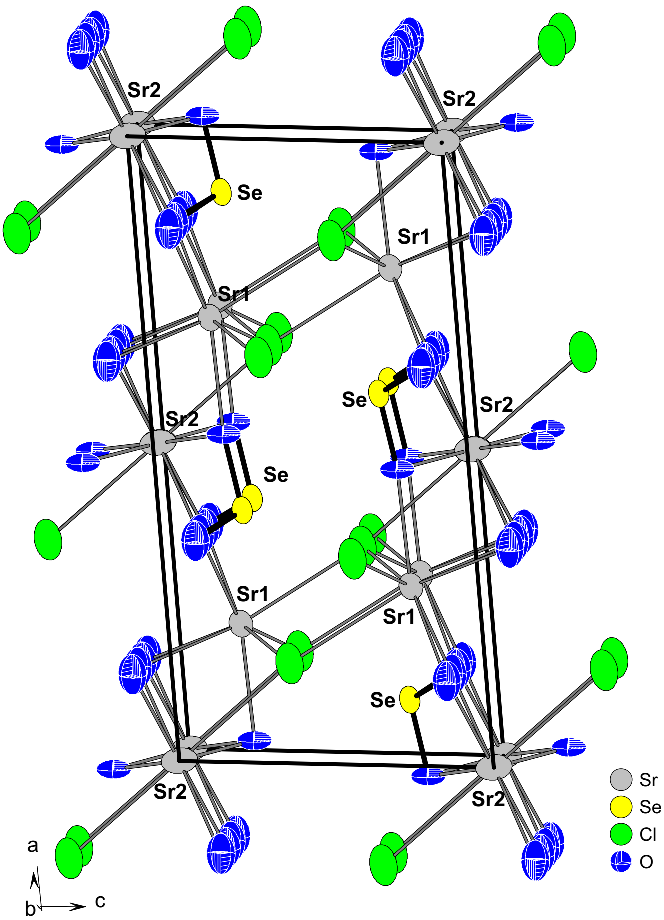

Fig. 2. View of $Sr_3(SeO_3)_2Cl_2$ crystal structure. A rectangle marks the unit cell.

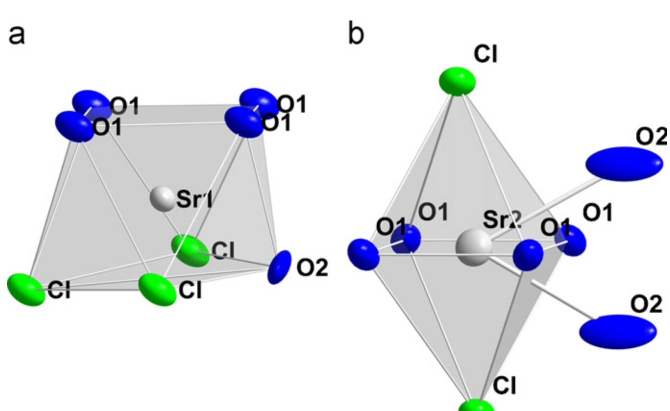

Fig. 3. Coordination polyhedra for Sr(1) (a) and Sr(2) (b) for the $Sr_3(SeO_3)_2Cl_2$ structure.

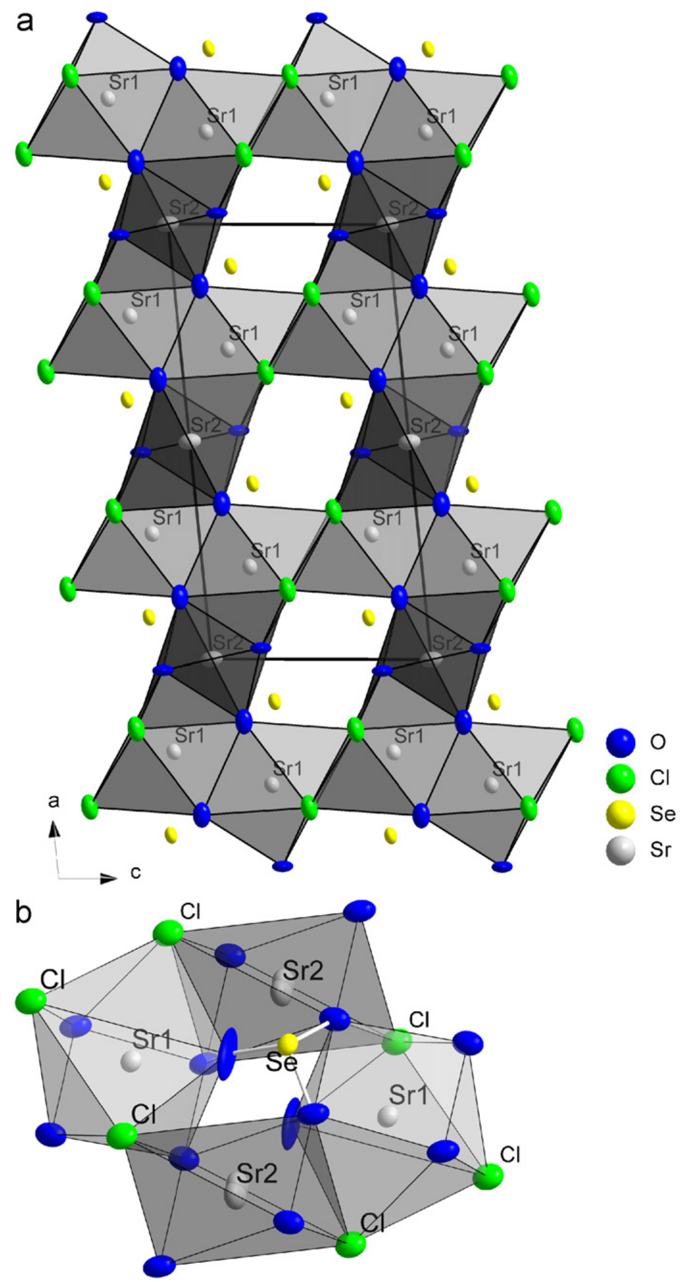

Fig. 4. The 3D framework with the channels in the $Sr_3(SeO_3)_2Cl_2$ crystal structure (a). Sr(2) polyhedra depicted as dark gray and Sr(1) as light gray. SeO_3 group in the $Sr_3(SeO_3)_2Cl_2$ structure (b).

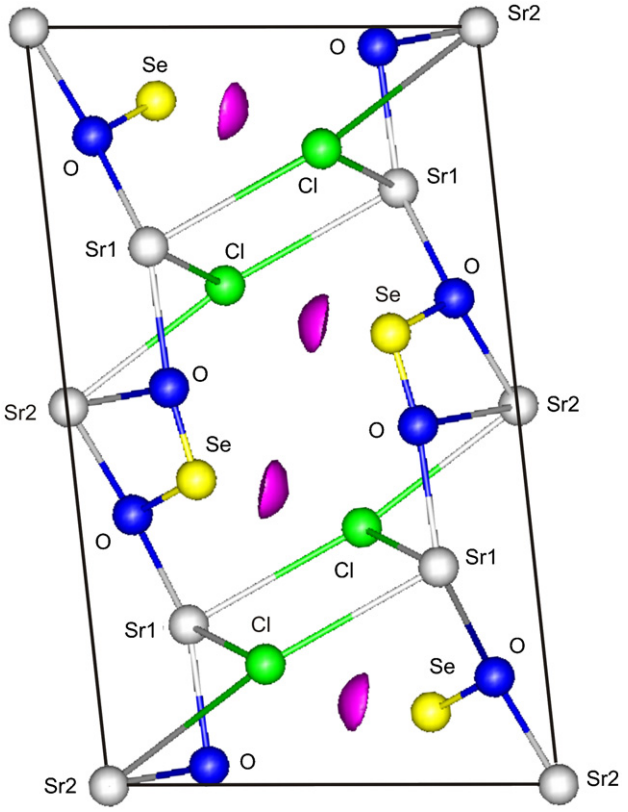

Fig. 5. The ELF isosurface at $\eta = 0.91$ for the $Sr_3(SeO_3)_2Cl_2$ unit cell.

Each $[Sr(1)O_5Cl_3]$ share edges with Sr1 polyhedra. As a result, the corrugated layer from Sr1 polyhedra exists parallel to *bc* plane of the unit cell. These layers are connected by $[Sr(2)O_{(4+2)}Cl_2]$, which share common edges with the Sr1 polyhedra from different layers. According to this description, the crystal structure of $Sr_3(SeO_3)_2Cl_2$ may be considered as a strontium polyhedra framework with channels (Fig. 4a). Selenium atoms are situated in the corners of these channels (Fig. 4a).

The coordination sphere of the Se atom is formed by three oxygen atoms (Table 3). Oxygen atoms and selenium atom form trigonal pyramids SeO_3. Taking into account the lone electron pair of Se(IV), selenium polyhedron may be described as a tetrahedron $[SeO_3E]$ with three oxygen vertices and one E. Such a coordination is usual for Se(IV). In the $Sr_3(SeO_3)_2Cl_2$ crystal structure the oxygen vertices of $[SeO_3E]$ belong to $[Sr(2)O_4Cl_2]$ and $[Sr(1)O_5Cl_3]$ polyhedra (Fig. 4b). This suggests that the lone electron pairs of Se(IV) must be pointed inside the channels in the $Sr_3(SeO_3)_2Cl_2$ structure.

The crystal structure of $Sr_3(SeO_3)_2Cl_2$ may be considered related to $Pb_3(SeO_3)_2Cl_2$ (C2/c, $a = 13.421$ Å, $b = 5.5809$ Å, $c = 13.0000$ Å, $\beta = 94.3^\circ$, $Z = 4$) [17]. The authors [17] select two different polyhedra for Pb1 and Pb2 ($[Pb(1)O_6Cl_2]$ and $[Pb(2)O_5Cl]$, respectively). The longest Pb–Cl distance in such description is 3.089 Å. *BVS* calculations for Pb(2) lead to only 1.68 whereas with two more distant chlorine atoms at 3.162 Å the *BVS* becomes 2.03. This fact allows to describe Pb(2) polyhedron as $[Pb(2)O_5Cl_3]$. The connection of Pb(1) and Pb(2) polyhedra in the $Pb_3(SeO_3)_2Cl_2$ structure forms a 3D framework with channels similar to those shown in Fig. 4a. The difference between $Sr_3(SeO_3)_2Cl_2$ and $Pb_3(SeO_3)_2Cl_2$ is the full occupance of the non-split of Metal(2) site (Pb2) which leads to the difference in the space group and to the doubling of the *c* cell constant.

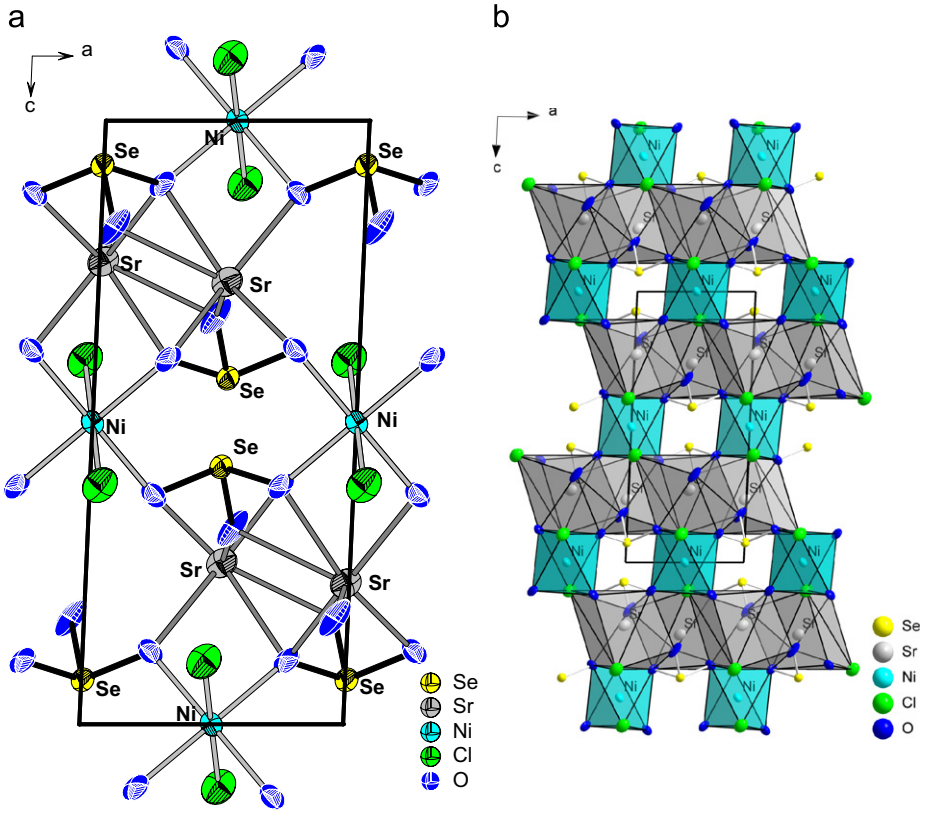

Fig. 6. The projection of the $Sr_3Ni(SeO_3)_2Cl_2$ crystal structure onto *ac* plane: (a) ortep view and (b) polyhedral presentation.

Since the asymmetric coordination of selenium atoms is often associated with the lone pair influence, we have performed a topological analysis of electron localization function (ELF) for the $Sr_3(SeO_3)_2Cl_2$ structure. The ELF analysis has proven to be a useful tool for locating such features.

An isosurface of ELF at $\eta = 0.91$ for the $SrSeO_3Cl_2$ unit cell is shown in Fig. 5. As may be seen from the figure, at high η values the first features to arise are the electron basins near the selenium atoms, evidently representing its 4*s* electron pairs. The shape of the basins is quite typical for the lone pairs that are considered stereochemically active. These lone pairs are pointed away from the Se–O bonds and into the channels in the structure. They are mostly located in the *ab* plane, however, being slightly tilted with respect to the *c* axis and not quite parallel to the *ab* plane. Further analysis of $\eta(r)$ down to $\eta = 0.88$ reveals no extra features, and after that the lowering of η leads to the appearance of atomic shells of Sr, O, and Cl, which is not accompanied by any changes in the topology of 4s-pairs of selenium that remains constant from $\eta = 0.91$ downwards. This result is in good agreement with our earlier assumption that the lone pairs of Se(IV) are pointed inside the channels in the $Sr_3(SeO_3)_2Cl_2$ structure.

As follows from our experimental results, one Sr atom in the $Sr_3(SeO_3)_2Cl_2$ crystal structure may be substituted by *d*-metal. Such substitution leads to a symmetry change (Table 1) but main structural features still remain the same.

The $Sr_2M(SeO_3)_2Cl_2$ (M = Co,Ni) phases are isostructural. In both structures Sr atoms are surrounded by six oxygen atoms and three chlorine atoms. The *BVS* calculations for such coordination utilizing data given in Table 3 and constants from [16] give values 1.93 for the Co compound and 1.94 for the Ni one. Cobalt and nickel are surrounded by octahedra formed by four oxygen atoms at the equatorial plane and two chlorine atoms in apical positions with the distances typical for M–O and M–Cl bonds (Table 3). Sr polyhedra are connected by common edges in *ab* plane. *d*-Metal atoms connect these layers into a 3D framework. Selenium atoms are situated at the corners of the channels of the framework. They are surrounded by oxygen atoms having SeO_3E tetrahedral coordination (Fig. 6).

The IR spectra of the new selenite chlorides presented in Fig. 1 show the usual absorption bands in ranges 884–856 and 752–760 cm^{-1} that can be assigned to the ν(Se–O) vibrations; bands in range 679–715 cm^{-1} originate from ν(Se–O–Sr) vibrations [9]. It may be noted that the spectra of $Sr_2M(SeO_3)_2Cl_2$ are more complex than $Sr_3(SeO_3)_2Cl_2$.

The substitution of strontium by barium atoms in the structure of $Sr_2Co(SeO_3)_2Cl_2$ leads to more symmetrical phase $Ba_2Co(SeO_3)_2Cl_2$ [18] (space group *P*/*nnm*, $a = 6.7635(4)$, $b = 12.6454(7)$, $c = 5.3866(3)$ Å). The principle of construction of this phase is the same as for compounds under investigation. $[BaO_7Cl_3]$ polyhedra sharing their common faces form infinite layers. These layers are connected by $[CoO_4Cl_2]$ octahedra into a 3D framework with channels where Se atoms are situated.

As it was expected, the presence of Se(IV) in the structure leads to the open 3D framework formation for all the investigated compounds. However, all the compounds have centrosymmetric structures regardless of the strontium substitution by *d*-metal atoms. It is known from literature that selenite chloride with composition $Cu_3(SeO_3)_2Cl_2$ exist in two forms [19,20]. But the crystal structures of $Cu_3(SeO_3)_2Cl_2$ are different from the structures of the compounds described in the presented work. From this point of view it would be interesting to obtain a compound containing both Sr and Cu^{2+} at the same time, which is the subject of our ongoing investigations.

Acknowledgments

Dr. T.B. Shatalova and Mrs. I.V. Kolesnik are gratefully acknowledged for assistance in thermal and IR analysis data collection. Presented work was supported by RFBR Grant 06-03-32134.

References

[1] C.N.R. Rao, J.N. Behera, M. Dan, Chem. Soc. Rev. 35 (2006) 375–387.
[2] P.S. Halasyamani, K.R. Poeppelmeier, Chem. Mater. 10 (1998) 2753–2769.
[3] M.S. Wickleder, Handbook on the Physics and Chemistry of Rare Earths 35 (2005) 45–105.
[4] R. Becker, M. Prester, H. Berger, P.H. Lin, M. Johnsson, D. Drobac, I. Zivkovic, J. Solid State Chem. 180 (2007) 1051–1059.
[5] Y.-L. Shen, J.-G. Mao, H.-L. Jiang, J. Solid State Chem. 178 (2005) 2942–2946.
[6] P. Millet, B. Bastide, V. Pashchenko, S. Gnatchenko, V. Gapon, Y. Ksari, A. Stepanov, J. Mater. Chem. 11 (2001) 1152–1157.
[7] R. Becker, M. Johnsson, Solid State Sci. 7 (2005) 375–380.
[8] O.A. Dityatiev, P. Lightfoot, P.S. Berdonosov, V.A. Dolgikh, Acta Cryst. E 63 (2007) i149–i150.
[9] H.-L. Jiang, J.-G. Mao, J. Solid State Chem. 181 (2008) 345–354.
[10] The International Centre for Diffraction Data 12 Campus Boulevard Newtown Square, PA 19073–3273 USA 〈http://www.icdd.com〉 PDF2 2001.
[11] G.M. Sheldrick, Acta Cryst. A 64 (2008) 112–122.
[12] C. Pisani, R. Dovesi, C. Roetti, HF ab-initio treatment of crystalline systems. Lecture notes in Chemistry, vol. 48; Springer, Berlin, 1988;
V.R. Saunders, R. Dovesi, C. Roetti, M. Causa, N.M. Harrison, R. Orlando, C.M. Zicovich-Wilson, CRYSTAL98, University of Torino, Torino, 1998.
[13] M.P. Habas, R. Dovesi, A. Lichanot, J. Phys. Cond. Matter 10 (1998) 6897–6909.
[14] C. Gatti, TOPOND98 User's Manual, CNR-CSRSRC, Milano, 1999.
[15] L. Laaksonen, J. Mol. Graphics 10 (1992) 33;
D.L. Bergman, L. Laaksonen, A. Laaksonen, J. Mol. Graphics Modelling 15 (1997) 301.
[16] I.D. Brown, Bond valence sum parameters version 2006–05–02. 〈http://www.ccp14.ac.uk/ccp/web-mirrors/i_d_brown/bond_valence_param/bvparm2006.cif〉.
[17] Y. Porter, P.S. Halasyamani, Inorg. Chem. 40 (2001) 2640–2641.
[18] M.G. Johnston, W.T.A. Harrison, Acta Cryst. E 58 (2002) i49–i51.
[19] P. Millet, B. Bastide, M. Johnsson, Solid State Commun. 113 (2000) 719–723.
[20] R. Becker, H. Berger, M. Johnsson, Acta Cryst. C 63 (2007) i4–i6.